SUPPORTING INFORMATION

ADDITIONAL DATA

Environment, Stability and Acidity of External Surface Sites of Silicalite-1 and ZSM-5 Micro- and Nano-Slabs, -Sheets and -Crystals

Laureline Treps,[†] Axel Gomez,[†,§] Theodorus de Bruin,[‡] Céline Chizallet[†,*]

[†] IFP Energies Nouvelles, Rond-point de l'échangeur, BP3, 69360 Solaize, France

[‡] IFP Energies Nouvelles, 1 et 4 avenue de Bois-Préau, BP3, 92852 Rueil-Malmaison, France

[§] Département de Chimie, École Normale Supérieure, PSL University, 75005 Paris, France

celine.chizallet@ifpen.fr

SI. Variation of the cleavage height for each surface orientation

For each investigated cleavage direction, a set of cleavage height was studied as illustrated in Figure S1.

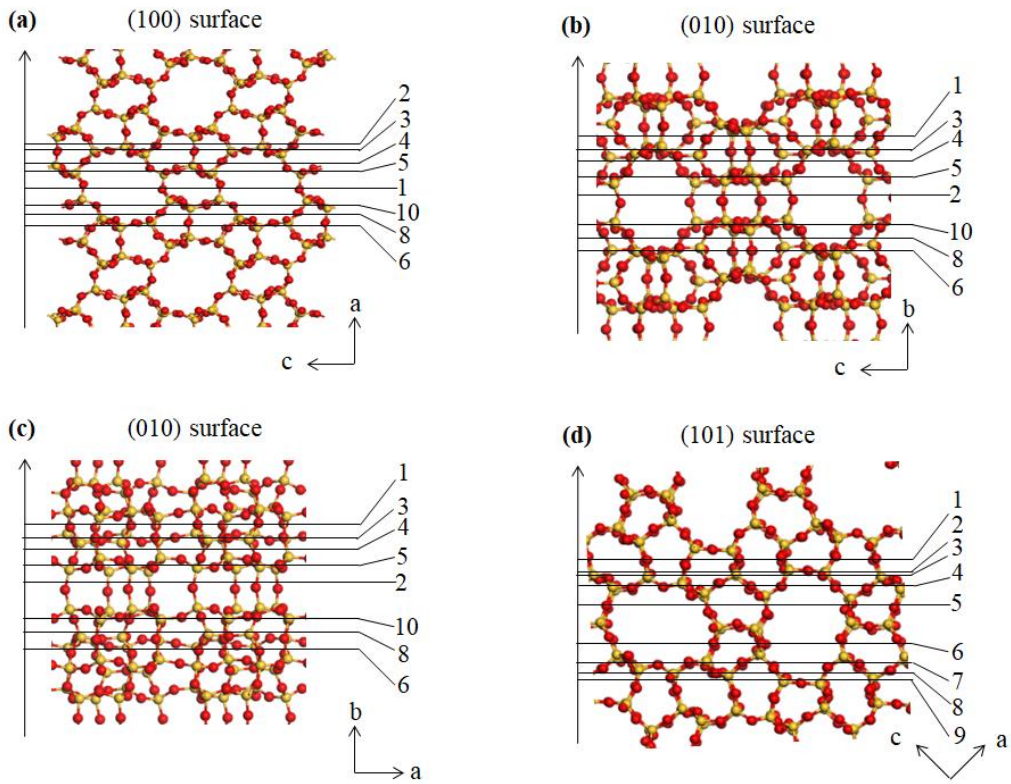

Figure S1. Different heights of cleavage along the (a) (100), (b) and (c) (010) and (d) (101) directions and their names (red: oxygen atoms; yellow: silicon atoms).

For the (100) surface orientation, cleavage 1 and 2 can generate a cell with a fractional thickness of 2 bulk units (see section SII) with symmetric surfaces. The others are non-symmetric for the same fractional thickness, it generates a cell with two different surfaces with the following association: 3/6, 4/8 and 5/10. To generate a symmetric cell with these last cleavages, the thickness was set smaller than 2. Figure S2 depicts side views of most important cleavages for each surface orientations.

The surface energies generated by the two methods are almost the same (Table S1) but the symmetric cell allows to calculate the individual surface energies. There is no substantial difference in energy when a dipolar correction is added (Table S1), so that such corrections were not applied in the following. For the (010) orientation, the same kind of approach led to asymmetric slabs in the 6/3, 8/4 and 10/5 cases. For the (101) surface orientation, the thickness is limited to a single cell for cleavage 1, because in this orientation the lateral dimensions of the cell are larger than for the two other surface orientations. The other cleavages are made symmetric by adjusting the thickness.

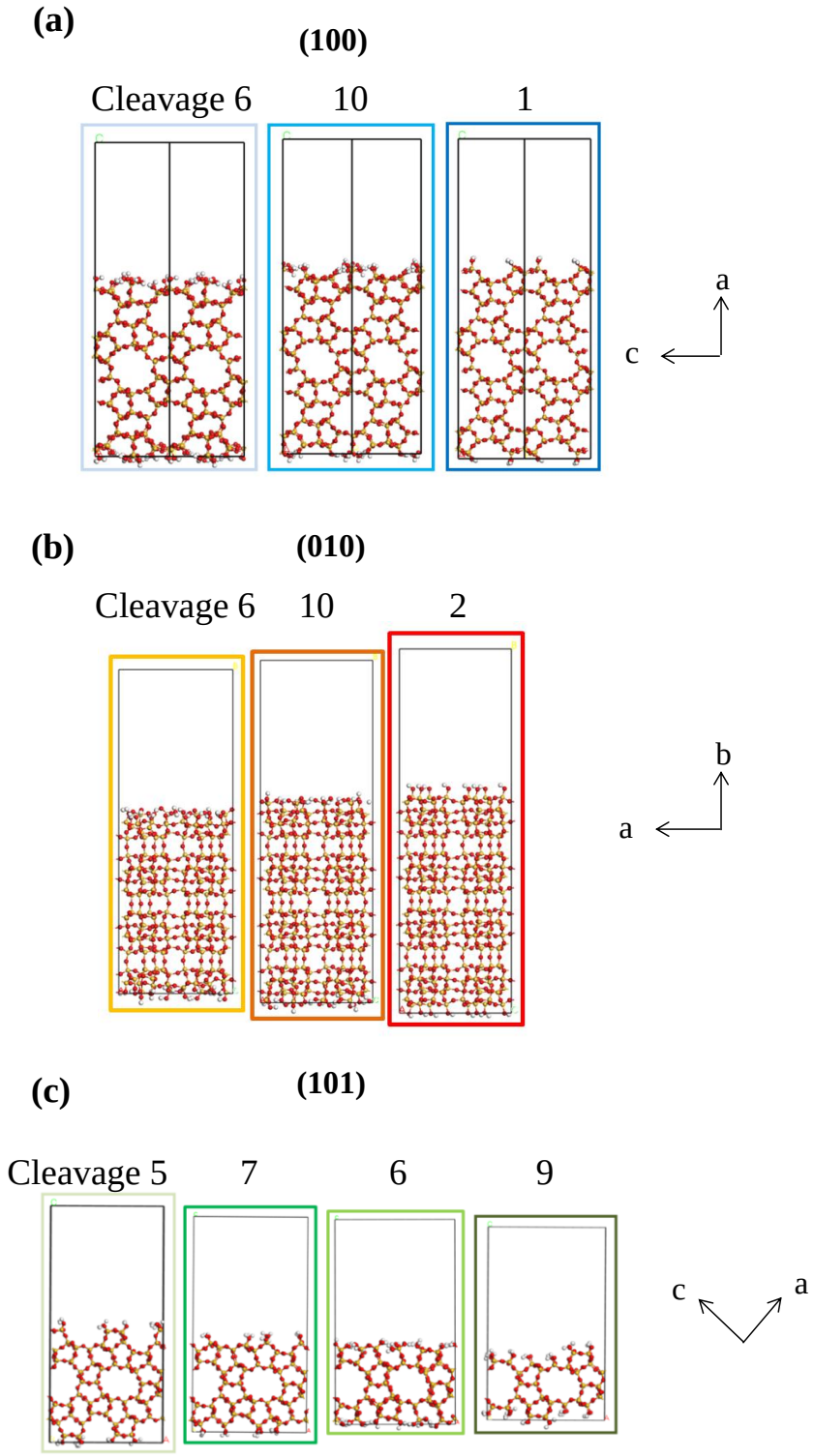

Figure S2. Side views of the simulation cells for the (a) (100), (b) (010) and (c) (101) surface orientations, at various cleavages.

Table S1. Surface free energies at 0 K for cleavages (CLV) along different surfaces: (100), (010) and (101). The most stable terminations according to the thermodynamic analysis are reported in bold.

(100)	θ_{H2O} (nm^{-2})	γ_{surf} ($J.m^{-2}$)	(010)	θ_{H2O} (nm^{-2})	γ_{surf} ($J.m^{-2}$)	(101)	θ_{H2O} (nm^{-2})	γ_{surf} ($J.m^{-2}$)
CLV1	**1.50**	**0.037**	CLV1	3.01	0.0239	CLV1	2,92	0.0001
CLV2	3.00	-0.001	**CLV2**	**1.50**	**0.0412**	CLV2	2.71	0.0257
CLV3	4.11	-0.064	CLV3	4.51	-0.1091	CLV3	3.54	-0.0438
CLV4	2.25	0.031	CLV4	2.26	0.0469	CLV4	3.75	-0.0735
CLV5	3.37	-0.052	CLV5	3.76	-0.0680	CLV5	1.88	0.0241
CLV6	4.11	-0.111	CLV6	4.51	-0.1258	**CLV6**	**1.88**	**0.0178**
CLV8	2.25	0.012	CLV8	2.26	0.0414	CLV7	3.75	-0.1412
CLV10	3.37	-0.098	CLV10	3.76	-0.1237	CLV8	3.54	-0.0841
CLV6/3	4.11	-0.109	CLV6/3	4.51	-0.1105	CLV9	2.71	-0.0252
CLV8/4	2.25	0.025	CLV8/4	2.26	0.0521			
CLV10/5	3.37	-0.069	CLV10/5	3.76	-0.0820			
CLV6/3 dipolar correction	4.11	-0.109						
CLV8/4 dipolar correction	2.25	0.025						
CLV10/5 dipolar correction	3.37	-0.069						

The surface energy variations are very low from one surface to the other, and mainly depends on the water coverage (water being in the form of Si-OH groups) (Figure S2).

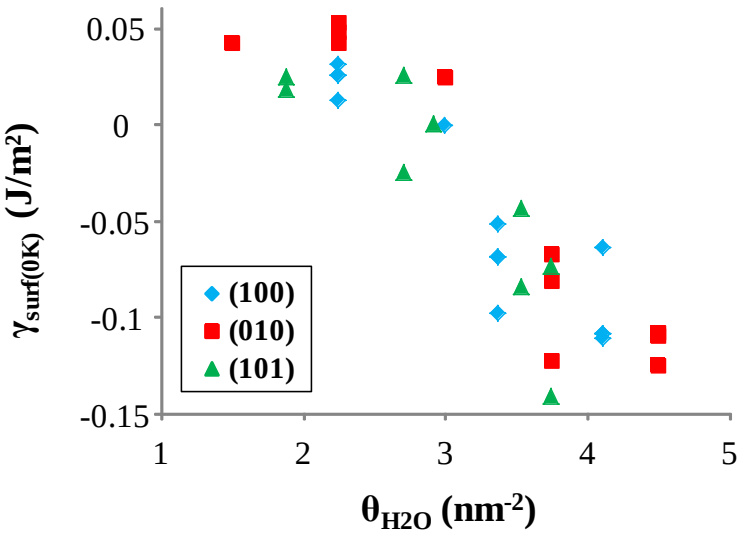

Figure S3. Evolution of the surface energy calculated at 0K function of the water coverage on each surface termination.

SII. Convergence of the calculated properties as a function of the slab thickness

The choice of the thickness of the slab model employed throughout the study is made thanks to a set of simulations for several thickness presented in Figure S4.

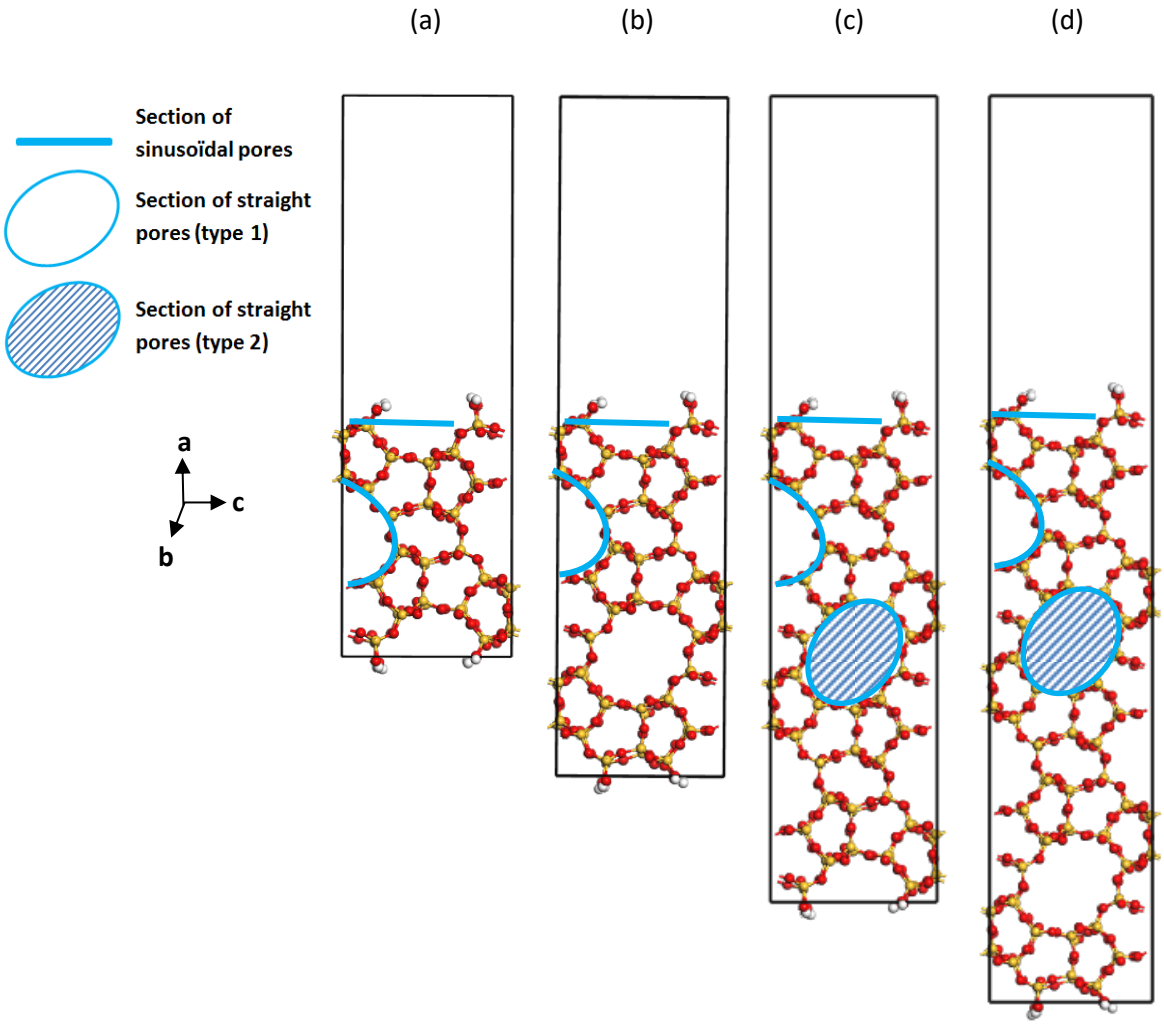

Figure S4. Side view of the investigated silicic slabs (cleavage (100)) at different height (bulk unit) along the a axis. Highlight of the measurement of the section area of the pores, the sinusoidal pore section is measured at the external surface whereas the straight pore sections are measured depending on the depth of the pore (type 1 close to the surface, type 2 deeper). Ellipse: straight pores along the b axis, green and black: sinusoidal pores along the a axis.

The dimensions of the pores are measured at the surface and in the layer (Figures S4 and S5). The dimensions of the pore in the middle of the cell should be as similar as possible as that of the bulk. A thickness of 2 bulk units in the a direction is a satisfactory compromise between accuracy and computational cost.

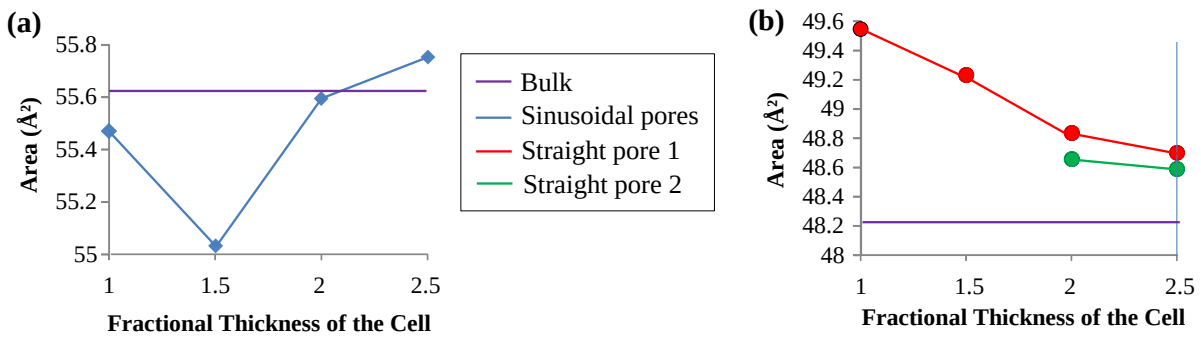

Figure S5. Area of the section of the (a) sinusoidal and (b) straight pores at the surface depending on the thickness of the model and compared to the similar pore of the bulk.

SIII. Surface free energies of the various surfaces

SIII.1. As a function of temperature, orientation by orientation

(a)

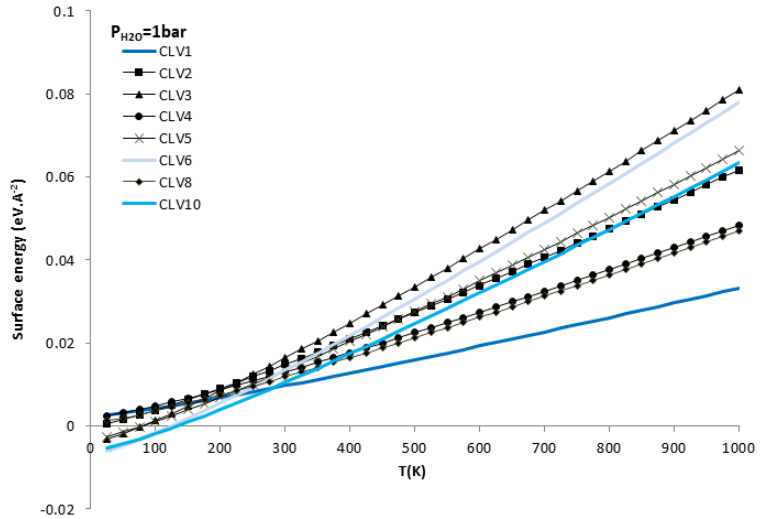

(b)

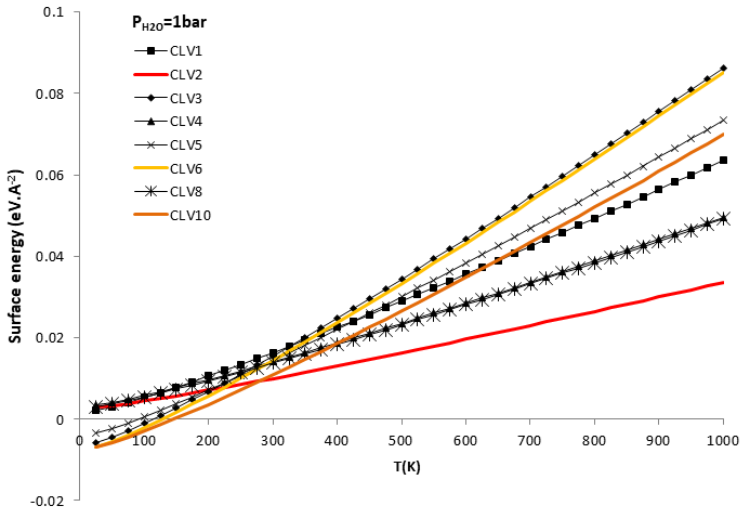

(c)

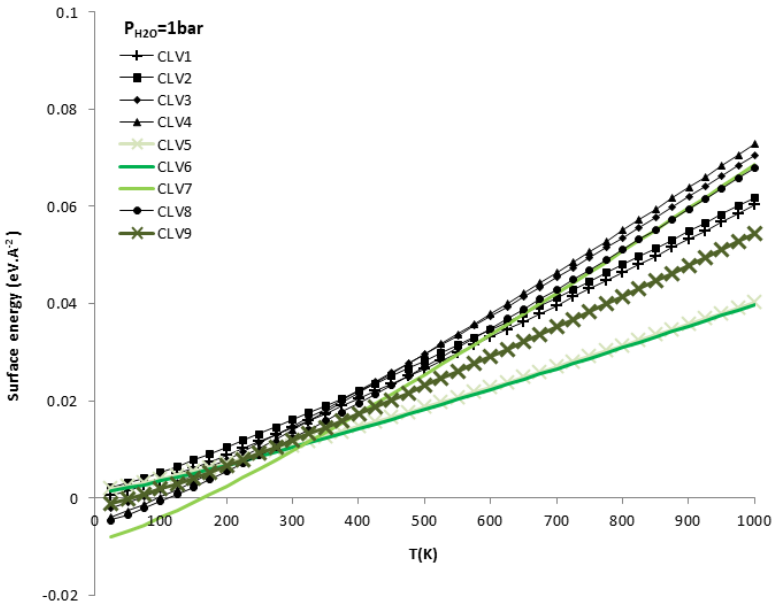

Figure S6. Evolution of the surface free energy as a function of the temperature for a water pressure of 1 bar, for all cleavage heights investigated in the (a) (100), (b) (010), (c) (101) orientations, including for cleavages that do not appear in the final thermodynamic diagram (Figure 2 in the manuscript).

SIII.2. Comparison of surface free energies for the various surfaces as a function of temperature

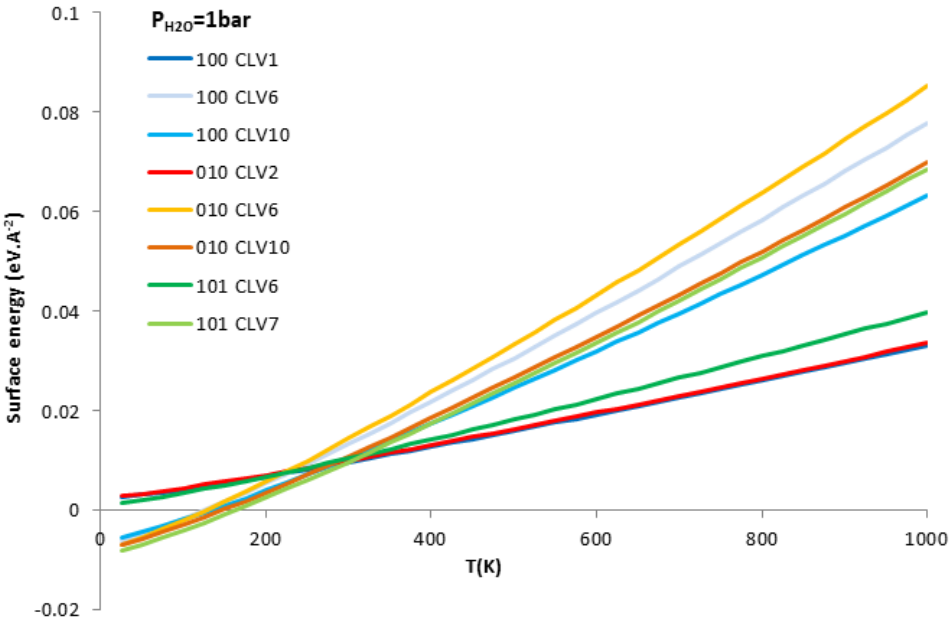

Figure S7. Evolution of the surface free energy as a function of the temperature for a water pressure of 1 bar, for the relevant cleavage heights appearing on the thermodynamic diagram (Figure 2 in the manuscript) of all surface orientations.

SIII.3. Effect of the explicit inclusion of the vibrational free energy for condensed phases

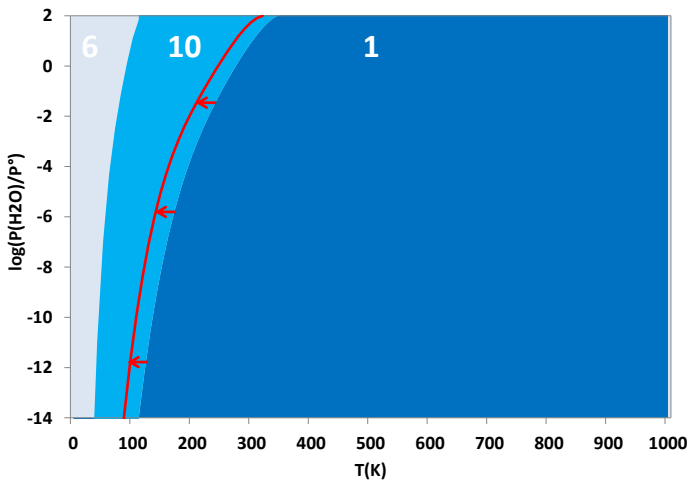

Figure S8. Effect of the consideration of vibrational free energies of condensed phase on the frontier separating the stability domain between cleavage 10 and 1 of the (100) surface (red line, other frontiers are drawn considering that the vibrational free energy of hydroxylated surfaces are the same as the equivalent number of gas phase water molecules and bulk silicalite-1, see Figure 2-a in the manuscript).

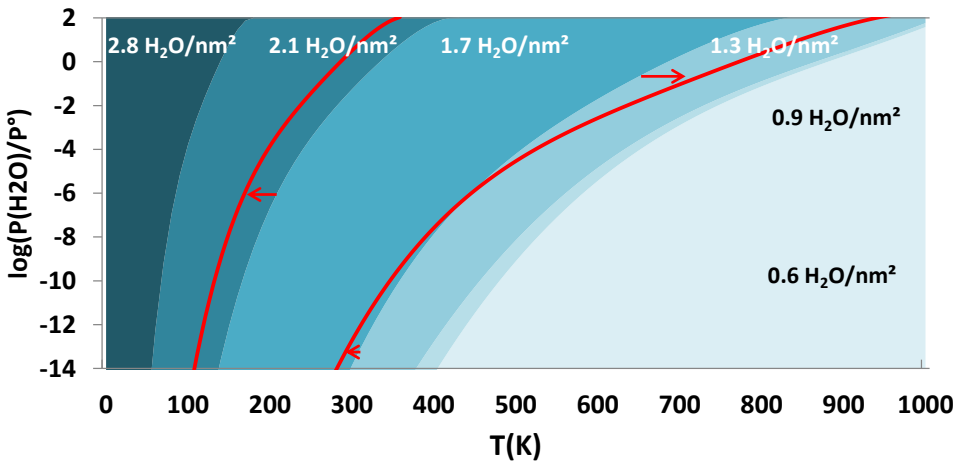

Figure S9. Effect of the consideration of vibrational free energies of condensed phase on the frontier separating the stability domain between various hydration states (2.1/1.7/1.3 H_2O/nm^2) of the aluminated (100) surface (cleavage 1, site n°59 is aluminated, see Figure 6-a in the manuscript).

SIV. Morphology constructions and comparison with experiments [1]

Gruene *et al*. performed (inter alia) TEM measurements for small monocrystalline silicalite-1 samples.[1] The reported dimensions were completed by other measurements (on the pictures, Figure S10), to allow a better comparison with our thermodynamic predictions (Figure 3).

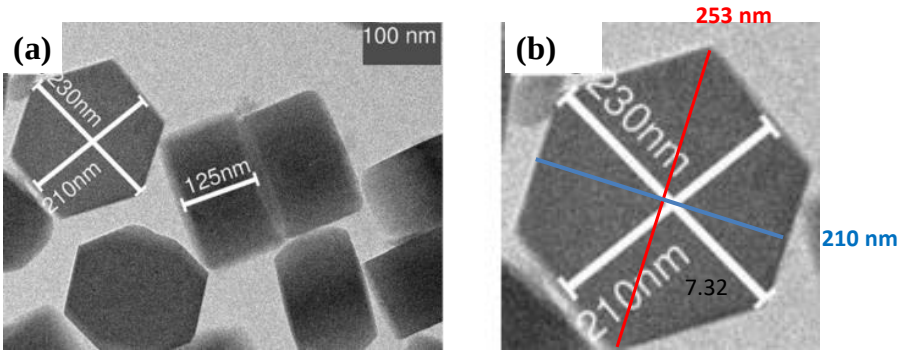

Figure S10. (a) TEM images of silicalite-1 crystals from ref.[1], (b) zoom on the particle analyzed for the measurements of the dimensions along the hexagonal projection. The colored dimensions were deduced from measurements on the screen. In red: longer dimension and blue: shorter dimension. Reprinted with permission of Wiley (Copyright 2018).

SV. Construction of surface model from the Si_{33} precursor species

Similarities between the models obtained by cleavage of the bulk structure and that obtained by assemblies of Si_{33} precursors are pointed out in Figure S11.

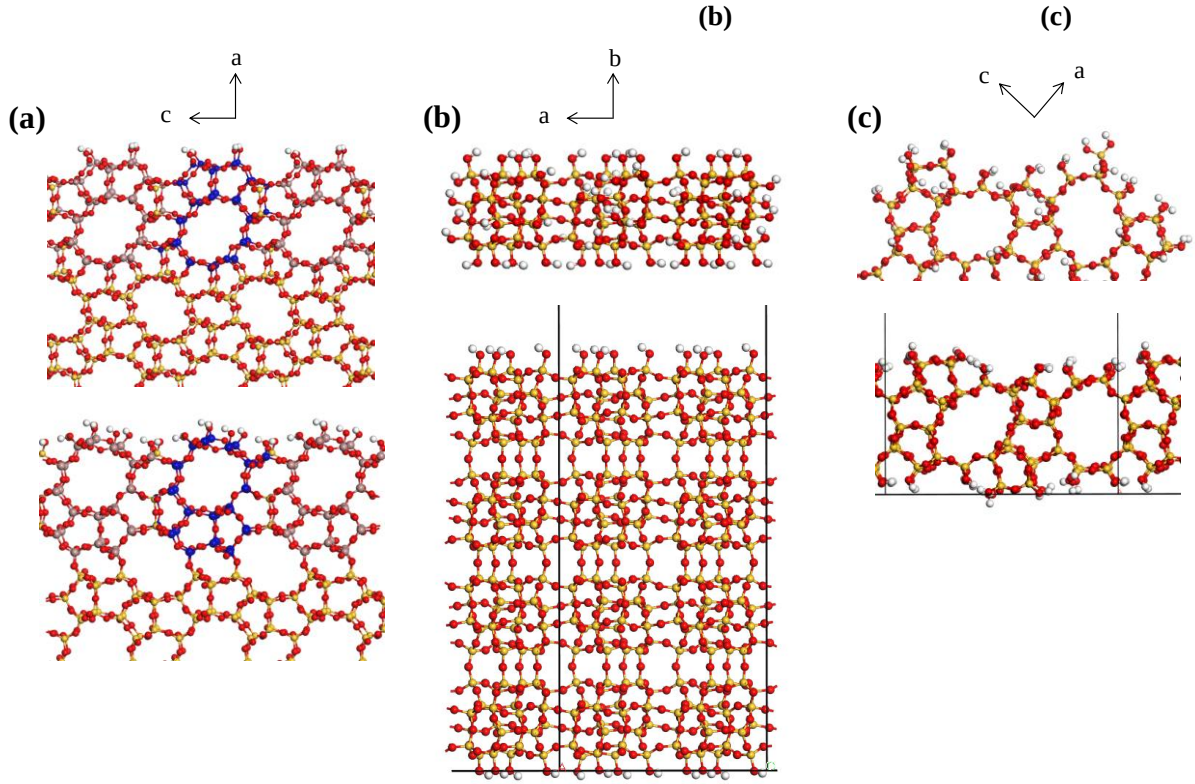

Figure S11. (a) Cleavage n°1 (top) and n°2 (bottom) for the (100) orientation, built by bulk cleavage. The Si atoms of the elementary Si_{33} units are emphasized in blue and grey for better visualization. (b) Analogy between the lateral view of a portion of the type 1 double nanoslab (top) and cleavage n°2 of the (010) surface (bottom). (c) approximate analogy between one of the lateral surface of the type 1 double nanoslab (top) and cleavage n°9 of the (101) surface (bottom).

SVI. Alumination energies

SVI.1. Alumination of the bulk sites

Table S2. Alumination energies (kJ.mol^{-1}) for bulk sites of the ZSM-5 T-sites. The terminology of the sites follows the one of IZA. Color code: Sinusoïdal chanel ; Straight chanel ; Intersection.

Al position	O position	$\Delta_r U_{al}$ (kJ.mol^{-1})		Al position	O position	$\Delta_r U_{al}$ (kJ.mol^{-1})
T1	O1	-22		T7	O16	-18
T1	O2	-24		T7	O18	-13
T1	O3	-26		T7	O11	-29
T1	O4	-11		T7	O17	-34
T2	O2	-22		T8	O17	-40
T2	O6	-32		T8	O19	-33
T2	O5	-27		T8	O6	-31
T2	O7	-31		T8	O20	-17
T3	O10	-44		T9	O15	-23
T3	O5	-26		T9	O21	-20
T3	O8	-29		T9	O19	-27
T3	O9	-9		T9	O22	-8
T4	O12	-28		T10	O24	-37
T4	O11	-37		T10	O3	-22
T4	O4	-19		T10	O23	-20
T4	O9	-8		T10	O22	-25
T5	O1	-18		T11	O16	-26
T5	O13	-28		T11	O25	-24
T5	O12	-13		T11	O14	-18
T5	O14	-19		T11	O24	-34
T6	O13	-24		T12	O25	-34
T6	O15	-14		T12	O8	-29
T6	O10	-26		T12	O26	-23
T6	O7	-18		T12	O20	-27

Li *et al*. also used DFT calculations to investigate the most stable T sites positions on the ZSM-5 bulk.[3] The relative energies of the T-sites of the bulk for a ratio of Si/Al=95 has been constructed to be compared to their model (Figure S12). Both sets of data are rather similar, the energies are in a 20 kJ.mol^{-1} interval, so the difference of stabilization for this Si/Al is not significant. Both studies find that the T-sites in the sinusoidal and straight pore are among the most stable sites. But we disagree on the order of stability for the T-site in the intersection. However, the energy difference is so weak that the differences could be included in the uncertainty of the DFT methods we use.

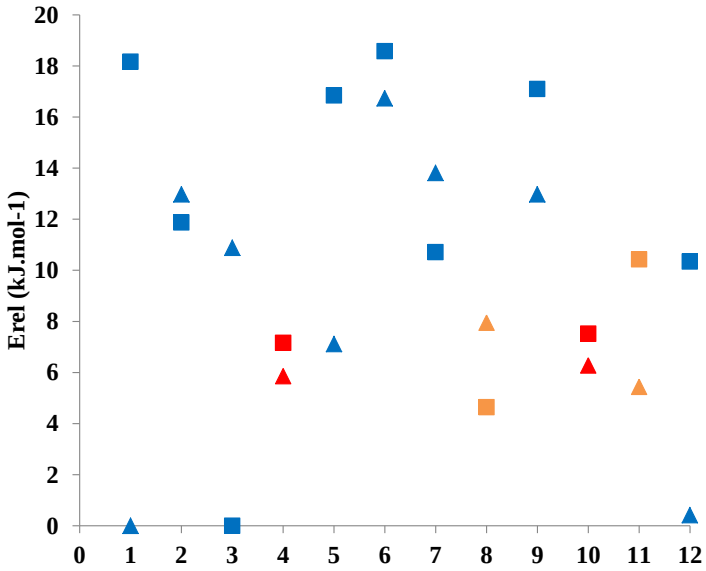

Figure S12. Relative alumination energies (kJ.mol^{-1}) of the different T-sites of the ZSM-5 bulk for Si/Al=95. T-sites at channel intersections are plotted in blue, whereas red and orange symbols correspond to T-sites within the sinusoidal and the straight channels respectively. T-sites are indicated by numbers corresponding the IZA attribution. Squares correspond to the results obtained in the present study whereas triangles correspond to data adapted from the study of Li *et al.*[3]

SVI.2. Alumination of the surface sites

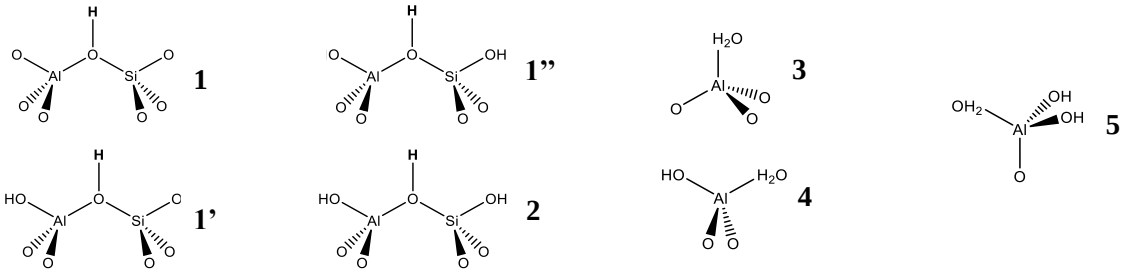

Figure S13. Nature of the surface acid sites associated to numbers for the legend of the following tables: Bridging Si-OH-Al, possibly close to Si-OH and/or Al-OH (1, 1’, 1” and 2), water molecules adsorbed on the aluminum, possibly close to Al-OH groups (3, 4 and 5).

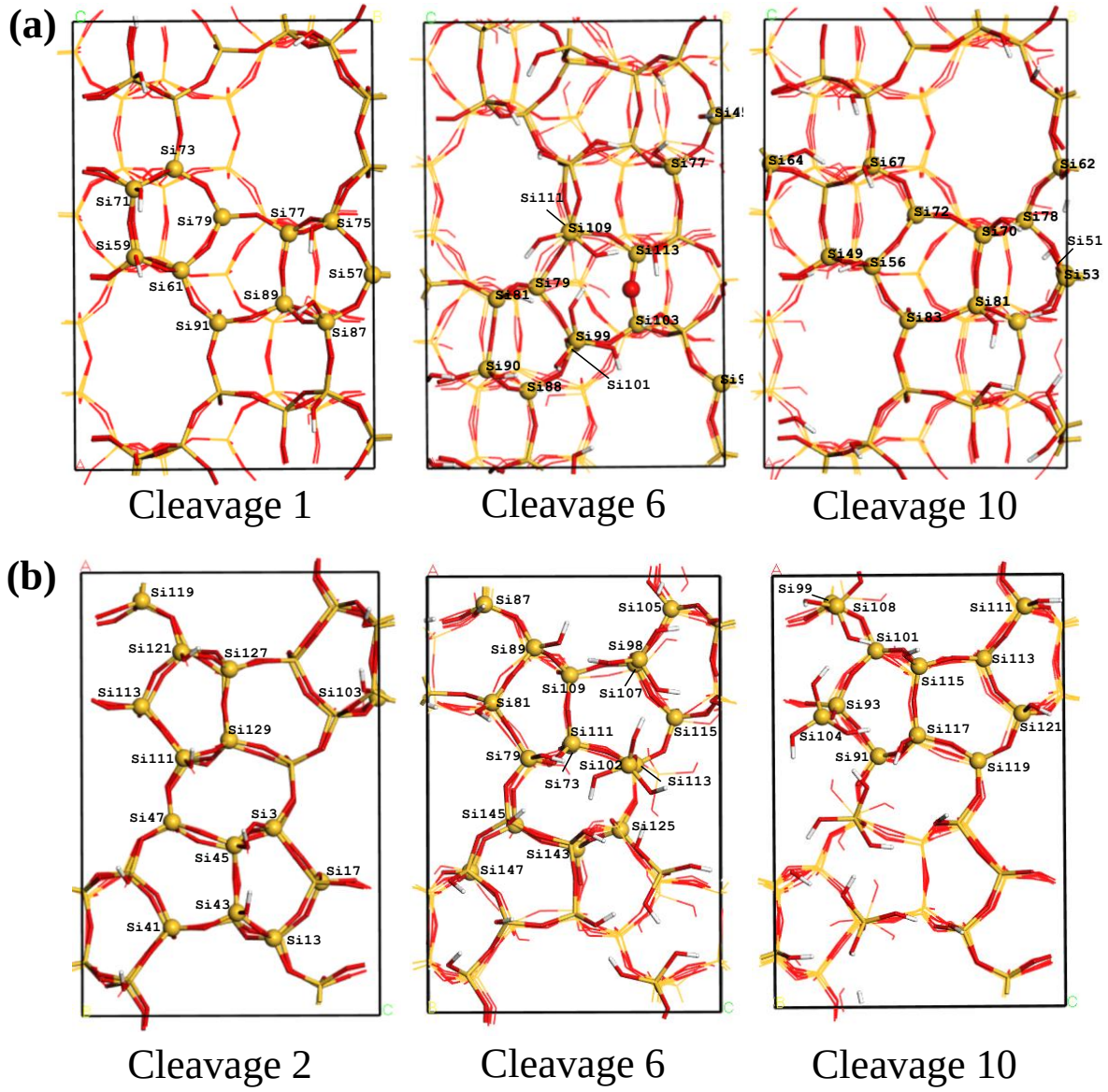

Figure S14. Top views of the most important surface cleavages, showing the numbering of the silicon atoms, on the (a) (100) and (b) (010) orientations.

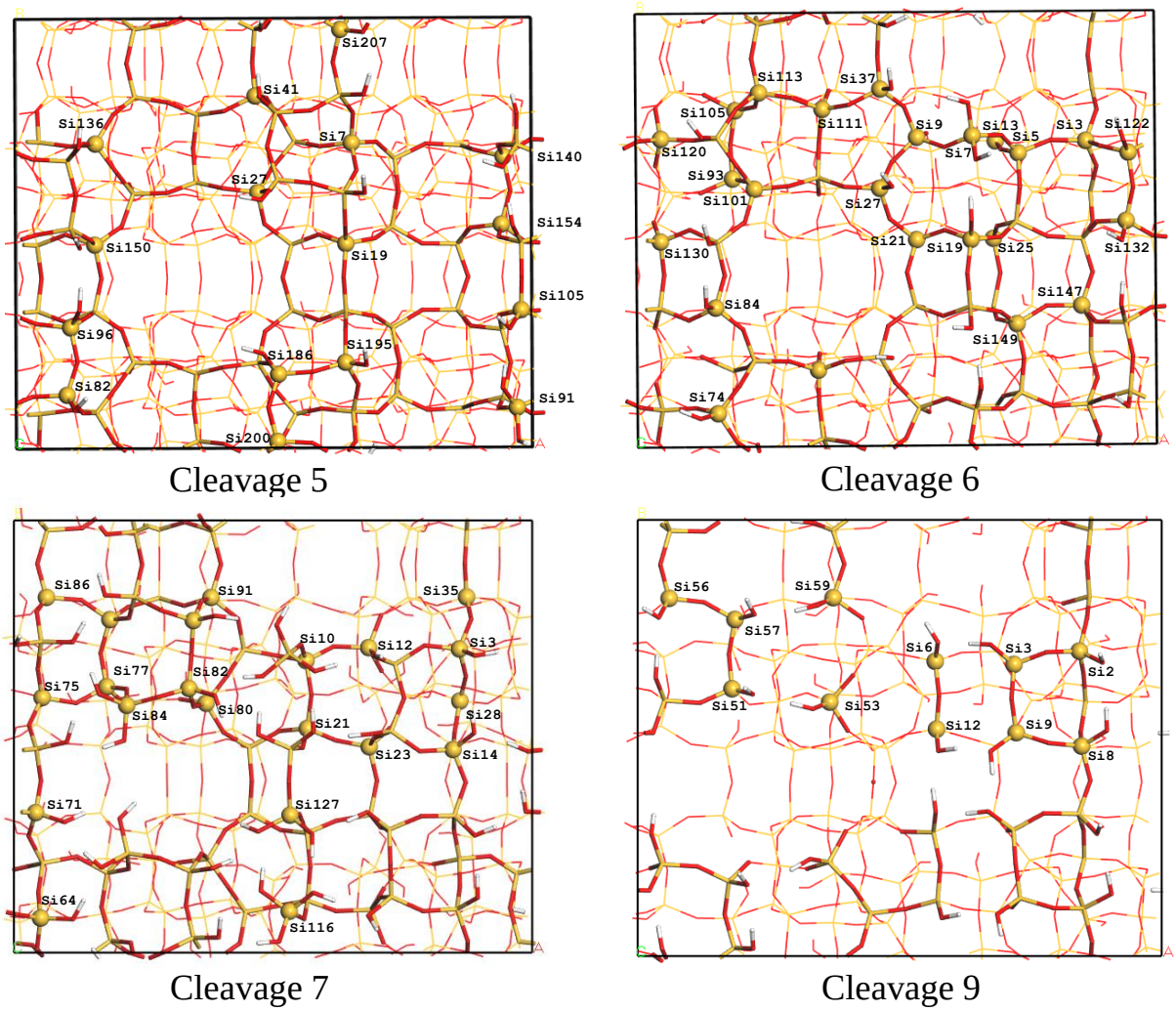

Figure S15. Top views of the most important surface cleavages, showing the numbering of the silicon atoms, on the (101) orientation.

Table S3. Alumination energy (kJ.mol^{-1}) for the slab model corresponding to cleavage 1 along (100). The types of site are defined in Figure S13. The aluminum position is shown in Figure S14. The same aluminum name can appear for different proton position due to the four oxygen surrounding the aluminum which could be studied here.

Type of site	Al position	$\Delta_r U_{al}$ (kJ.mol^{-1})
Bridging Si-OH-Al (Type 1)	Si_87	-52
	Si_79	-49
	Si_89	-46
	Si_89	-38
	Si_77	-37
	Si_61	-37
	Si_79	-35
	Si_77	-35
	Si_91	-34
	Si_79	-33
	Si_87	-33
	Si_73	-32
	Si_73	-30
	Si_69	-27
	Si_91	-27
	Si_77	-25
	Si_73	-25
	Si_91	-25
	Si_61	-23
	Si_61	-23
	Si_69	-20
	Si_89	-20
	Si_91	-15
	Si_79	-15
	Si_57	-15
Bridging Si-OH-Al (Type 1')	Si_75	-34
	Si_71	-23
	Si_71	-22
	Si_75	-22
	Si_59	-17
	Si_75	-14
	Si_59	-12
Bridging Si-OH-Al (Type 1")	Si_89	-51
	Si_69	-49
	Si_57	-46
	Si_73	-39
	Si_69	-39
	Si_77	-35
	Si_57	-33
	Si_57	-22
	Si_61	-21
Bridging Si-OH-Al (Type 2)	Si_59	-38
	Si_87	-25
	Si_71	-19
Al-H_2O (Type 3)	Si_75	-75
	Si_87	-68
	Si_71	-68
	Si_59	-57

Table S4. Alumination energy (kJ.mol^{-1}) for the slab model corresponding to cleavage 6 along (100). The types of site are defined in Figure S13. The aluminum position is shown in Figure S14.

Type of site	Al position	$\Delta_r U_{al}$ (kJ.mol^{-1})
Bridging Si-OH-Al (Type 1)	Si_101	-52
	Si_103	-43
	Si_79	-36
	Si_101	-36
	Si_101	-36
	Si_111	-35
	Si_103	-33
	Si_88	-33
	Si_88	-33
	Si_79	-32
	Si_113	-31
	Si_113	-29
	Si_111	-28
	Si_113	-27
	Si_103	-26
	Si_88	-25
	Si_111	-24
	Si_79	-19
Bridging Si-OH-Al (Type 1')	Si_77	-42
	Si_81	-33
	Si_90	-29
	Si_105	-23
	Si_109	-14
Bridging Si-OH-Al (Type 1")	Si_103	-41
	Si_111	-50
	Si_113	-38
	Si_79	-47
	Si_88	-48
	Si_101	-21
Bridging Si-OH-Al (Type 2)	Si_45	-69
	Si_45	-58
	Si_77	-55
	Si_105	-52
	Si_92	-46
	Si_109	-44
	Si_105	-38
	Si_45	-38
	Si_81	-38
	Si_81	-37
	Si_90	-37
	Si_77	-30
	Si_99	-29
	Si_92	-23
	Si_92	-18
	Si_90	-13
Al-H_2O (Type 3)	Si_77	-141
	Si_45	-127
	Si_92	-114
	Si_90	-101
	Si_81	-62
	Si_105	-57
Al-H_2O (Type 4)	Si_109	-79
	Si_109	-74
Al-H_2O (Type 5)	Si_99	-105
	Si_99	-82
	Si_99	-69

Table S5. Alumination energy (kJ.mol^{-1}) for the slab model corresponding to cleavage 10 along (100). The types of site are defined in Figure S13. The aluminum position is shown in Figure S14.

Type of site	Al position	$\Delta_r U_{al}$ (kJ.mol^{-1})
Bridging Si-OH-Al (Type 1)	Si_49	-56
	Si_51	-53
	Si_62	-45
	Si_49	-41
	Si_49	-41
	Si_62	-40
	Si_83	-33
	Si_83	-29
	Si_51	-26
	Si_78	-23
	Si_78	-19
	Si_62	-17
	Si_51	-17
	Si_72	-17
	Si_78	-16
Bridging Si-OH-Al (Type 1')	Si_67	-81
	Si_56	-59
	Si_70	-51
	Si_67	-36
	Si_56	-32
	Si_81	-31
	Si_70	-27
	Si_81	-22
	Si_64	-20
	Si_56	-16
	Si_53	1
Bridging Si-OH-Al (Type 1")	Si_62	-85
	Si_78	-47
	Si_49	-40
	Si_72	-40
	Si_72	-40
	Si_83	-39
	Si_72	-35
	Si_51	-24
	Si_83	-22
Bridging Si-OH-Al (Type 2)	Si_67	-35
	Si_81	-18
	Si_64	-5
	Si_70	1
Al-H_2O (Type 3)	Si_67	-102
	Si_70	-99
	Si_56	-84
	Si_81	-54
Al-H_2O (Type 4)	Si_64	-96
	Si_64	-71
Al-H_2O (Type 5)	Si_53	-86
	Si_53	-70
	Si_53	-33

Table S6. Alumination energy (kJ.mol^{-1}) for the slab model corresponding to cleavage 2 along (010). The types of site are defined in Figure S13. The aluminum position is shown in Figure S14.

Type of site	Al position	$\Delta_r U_{al}$ (kJ.mol^{-1})
Bridging Si-OH-Al (Type 1)	Si_103	-46
	Si_17	-42
	Si_127	-39
	Si_17	-32
	Si_113	-32
	Si_41	-32
	Si_17	-31
	Si_13	-27
	Si_47	-26
	Si_103	-26
	Si_3	-26
	Si_103	-25
	Si_129	-25
	Si_119	-25
	Si_17	-22
	Si_13	-20
	Si_127	-19
	Si_129	-19
	Si_3	-18
	Si_3	-14
	Si_103	-11
	Si_13	-9
	Si_129	-9
	Si_127	-8
Bridging Si-OH-Al (Type 1')	Si_45	-22
	Si_121	-18
	Si_111	-17
	Si_45	-16
	Si_121	-15
	Si_121	-14
	Si_111	-13
	Si_111	-9
	Si_43	-3
	Si_43	-1
Bridging Si-OH-Al (Type 1")	Si_113	-42
	Si_41	-36
	Si_47	-35
	Si_113	-34
	Si_119 / T5	-34
	Si_129 / T3	-34
	Si_119	-30
	Si_47 / T11	-29
	Si_41	-28
	Si_41 / T8	-27
	Si_113 / T2	-26
	Si_3 / T1	-24
	Si_119	-23
	Si_127 / T4	-22
	Si_47	-22
	Si_13 / T6	-17
Bridging Si-OH-Al (Type 2)	Si_43	-26
	Si_45	-21
Al-H_2O (Type 3)	Si_43 / T9	-59
	Si_45 / T10	-58
	Si_111 / T7	-43
	Si_121 / T12	-35

Table S7. Alumination energy (kJ.mol^{-1}) for the slab model corresponding to cleavage 6 along (010). The types of site are defined in Figure S13. The aluminum position is shown in Figure S14.

Type of site	Al position	$\Delta_r U_{al}$ (kJ.mol^{-1})
Bridging Si-OH-Al (Type 1)	Si_111	-48
	Si_73	-44
	Si_111	-42
	Si_125	-41
	Si_143	-40
	Si_73	-39
	Si_125	-34
	Si_73	-34
	Si_73	-33
	Si_145	-32
	Si_143	-32
	Si_111	-30
	Si_125	-29
	Si_147	-27
	Si_125	-26
	Si_147	-25
	Si_143	-23
	Si_145	-23
	Si_147	-23
	Si_145	-22
	Si_145	-22
	Si_147	-17
	Si_143	-10
Bridging Si-OH-Al (Type 1')	Si_98	-42
	Si_89	-39
	Si_102	-17
	Si_79	-16
Bridging Si-OH-Al (Type 1")	Si_107	-68
	Si_113	-57
	Si_111	-52
	Si_109	-39
	Si_105	-29
	Si_115	-22
Bridging Si-OH-Al (Type 2)	Si_87	-55
	Si_81	-47
	Si_87	-45
	Si_81	-40
	Si_79	-32
	Si_89	-27
	Si_89	-26
	Si_87	-21
	Si_81	-18
	Si_79	-17
Al-H_2O (Type 3)	Si_89	-113
	Si_79	-97
	Si_81	-73
	Si_87	-64
Al-H_2O (Type 5)	Si_102	-90
	Si_98	-80
	Si_98	-75
	Si_98	-73
	Si_102	-32
	Si_102	9

Table S8. Alumination energy (kJ.mol^{-1}) for the slab model corresponding to cleavage 10 along (010). The types of site are defined in Figure S13. The aluminum position is shown in Figure S14.

Type of site	Al position	$\Delta_r U_{al}$ (kJ.mol^{-1})
Bridging Si-OH-Al (Type 1)	Si_93	-41
	Si_91	-36
	Si_101	-36
	Si_93	-32
	Si_101	-32
	Si_93	-27
	Si_99	-26
	Si_91	-25
	Si_99	-22
	Si_101	-22
	Si_91	-21
	Si_119	-21
	Si_99	-19
	Si_113	-11
Bridging Si-OH-Al (Type 1')	Si_111	-44
	Si_115	-33
	Si_115	-31
	Si_121	-20
	Si_117	-17
	Si_117	-16
	Si_108	-9
	Si_111	-9
	Si_121	-7
	Si_104	-4
	Si_121	-4
	Si_111	9
Bridging Si-OH-Al (Type 1")	Si_113	-52
	Si_99	-43
	Si_119	-43
	Si_119	-43
	Si_113	-41
	Si_93	-24
	Si_101	-16
	Si_91	-14
	Si_119	-8
	Si_113	-4
Bridging Si-OH-Al (Type 2)	Si_115	-6
	Si_117	2
Al-H_2O (Type 3)	Si_111	-100
	Si_117	-89
	Si_121	-87
	Si_115	-4
Al-H_2O (Type 5)	Si_104	-104
	Si_104	-99
	Si_108	-94
	Si_108	-47
	Si_108	-42
	Si_104	-30

Table S9. Alumination energy (kJ.mol^{-1}) for the slab model corresponding to cleavage 5 along (101). The types of site are defined in Figure S13. The aluminum position is shown in Figure S15.

Type of site	Al position	$\Delta_r U_{al}$ (kJ.mol^{-1})
Bridging Si-OH-Al (Type 1)	Si_136	-48
	Si_150	-40
	Si_19	-39
	Si_27	-38
	Si_140	-38
	Si_7	-38
	Si_41	-36
	Si_7	-33
	Si_154	-29
Bridging Si-OH-Al (Type 1')	Si_200	-55
	Si_105	-43
	Si_195	-38
	Si_195	-35
	Si_207	-33
	Si_186	-32
	Si_96	-24
	Si_82	-23
	Si_91	0
Bridging Si-OH-Al (Type 1")	Si_7	-60
	Si_41	-56
	Si_7	-53
	Si_19	-52
	Si_154	-46
	Si_27	-44
	Si_136	-34
	Si_140	-33
	Si_150	-10
Bridging Si-OH-Al (Type 2)	Si_82	-70
	Si_105	-59
	Si_200	-54
	Si_207	-52
	Si_96	-43
	Si_200	-43
	Si_186	-41
	Si_105	-35
	Si_82	-34
	Si_195	-31
	Si_186	-28
	Si_96	-25
	Si_207	-24
	Si_91	2
Al-H_2O (Type 3)	Si_207	-91
	Si_96	-87
	Si_200	-87
	Si_105	-82
	Si_186	-69
	Si_82	-64
	Si_195	-63
Al-H_2O (Type 4)	Si_91	-71
	Si_91	-45

Table S10. Alumination energy (kJ.mol^{-1}) for the slab model corresponding to cleavage 6 along (101). The types of site are defined in Figure S13. The aluminum position is shown in Figure S15.

Type of site	Al position	$\Delta_r U_{al}$ (kJ.mol^{-1})
Bridging Si-OH-Al (Type 1)	Si_5	-61
	Si_149	-55
	Si_55	-54
	Si_13	-53
	Si_25 / T12	-53
	Si_55	-52
	Si 149 / T8	-50
	Si_111 / T11	-44
	Si_149	-44
	Si_5	-44
	Si_147	-42
	Si_3	-41
	Si_120	-40
	Si_105	-38
	Si_105	-38
	Si_93	-38
	Si_3	-37
	Si_105 / T8	-36
	Si_55 / T5	-35
	Si_147	-35
	Si_93 / T2	-34
	Si_3 / T1	-33
	Si_111	-33
	Si_25 / T12	-32
	Si_13 / T6	-32
	Si_113 / T12	-32
	Si_93	-31
	Si_130	-31
	Si_113	-31
	Si_130 /T10	-30
	Si_101 / T6	-29
	Si_111	-28
	Si_25	-28
	Si_113	-27
	Si_25	-26
	Si_9	-26
	Si_93	-25
	Si_5 / T2	-25
	Si_21	-25
	Si_120 / T4	-24
	Si_105	-23
	Si_21	-22
	Si_13	-22
	Si_147	-21
	Si_13	-21
	Si_101 / T6	-20
Bridging Si-OH-Al (Type 1')	Si_37	-52
	Si_132	-40
	Si_7	-36
	Si_122	-32
	Si_37	-31
	Si_132	-31
	Si_74	-28
	Si_122	-23
	Si_84	-21

	Si_74	-18
	Si_19	-16
	Si_84	-15
	Si_7	-13
	Si_27	-11
	Si_27	-11
	Si_27	-5
	Si_74	-4
	Si_19	32
Bridging Si-OH-Al (Type 1”)	Si_21 / T10	-45
	Si_5	-42
	Si_149	-41
	Si_120	-39
	Si_9 / T4	-38
	Si_147 / T7	-34
	Si_130	-33
	Si_113	-32
	Si_9	-30
	Si_130	-29
	Si_55	-28
	Si_3	-28
	Si_9	-27
	Si_111	-26
	Si_120	-22
	Si_21	-21
	Si_101	-20
	Si_101 / T6	-19
Bridging Si-OH-Al (Type 2)	Si_37	-33
	Si_132	-19
	Si_122	-18
	Si_19	-7
	Si_84	-5
Al-H_2O (Type 3)	Si_37 / T7	-75
	Si_132 / T5	-75
	Si_84 / T9	-72
	Si_19 / T9	-71
	Si_74 / T3	-59
	Si_122 / T11	-55
	Si_27 / T1	-48
Al-H_2O (Type 4)	Si_7 / T3	-57
	Si_7	-54

Table S11. Alumination energy (kJ.mol^{-1}) for the slab model corresponding to cleavage 7 along (101). The types of site are defined in Figure S13. The aluminum position is shown in Figure S15.

Type of site	Al position	$\Delta_r U_{al}$ (kJ.mol$^{-1)}$
Bridging Si-OH-Al (Type 1)	Si_80	-73
	Si_35	-51
	Si_28	-49
	Si_75	-42
	Si_23	-38
	Si_75	-35
	Si_12	-34
	Si_88	-34
	Si_91	-31
	Si_21	-29
	Si_77	-27
	Si_10	-25

	Si_86	-22
	Si_28	-8
Bridging Si-OH-Al (Type 1')	Si_127	-55
	Si_82	-49
	Si_14	-44
	Si_3	-39
	Si_93	-19
	Si_71	-18
	Si_84	-10
	Si_3	-9
	Si_116	-6
	Si_64	-3
	Si_64	18
Bridging Si-OH-Al (Type 1")	Si_77	-64
	Si_21	-63
	Si_80	-56
	Si_23	-55
	Si_88	-55
	Si_35	-47
	Si_28	-41
	Si_75	-40
	Si_12	-35
	Si_28	-34
	Si_91	-34
	Si_86	-30
	Si_10	-24
	Si_75	-16
Bridging Si-OH-Al (Type 2)	Si_14	-90
	Si_82	-48
	Si_93	-45
	Si_82	-40
	Si_71	-38
	Si_127	-35
	Si_14	-33
	Si_3	-29
	Si_93	-14
	Si_84	-5
Al-H_2O (Type 3)	Si_82	-102
	Si_3	-95
	Si_93	-75
	Si_14	-34
Al-H_2O (Type 4)	Si_127	-98
	Si_64	-87
	Si_127	-72
	Si_84	-70
	Si_71	-63
	Si_71	-57
	Si_84	-40
	Si_64	-37
Al-H_2O (Type 5)	Si_116	-59
	Si_116	-45
	Si_116	-35

Table S12. Alumination energy (kJ.mol^{-1}) for the slab model corresponding to cleavage 9 along (101). The types of site are defined in Figure S13. The aluminum position is shown in Figure S15.

Type of site	Al position	$\Delta_r U_{al}$ (kJ.mol^{-1})
Al-H_2O (Type 3)	Si_57	-110
	Si_59	-108
	Si_51	-91
	Si_8	-89
	Si_3	-88
	Si_53	-82
	Si_56	-79
	Si_2	-75
	Si_12	-66
	Si_9	-63
	Si_6	-60

Table S13. Comparison of the nature and stability of the most stable sites in bulk aluminated structures, when exposed on the three considered dominant surface orientations.

Most stable T-sites in the bulk	$\Delta_r U_{al}$ (kJ.mol^{-1}) in the bulk	Rank among (100) most stable surface sites (cleavage 1) / Nature of the site	Rank among (010) most stable surface sites (cleavage 2) / Nature of the site	Rank among (101) most stable surface sites (cleavage 6) / Nature of the site
T3	-44	9 / Al-OH-Si	13 / Al-OH-Si-OH	7 / Al-(H_2O)(OH) 6 / Al-H_2O
T8	-40	7 / Al-OH-Si-OH	8 / Al-OH-Si-OH	8 / Al-OH-Si
T4	-37	10 / Al-OH-Si-OH	7 / Al-OH-Si	26 / Al-OH-Si
T10	-37	8 / Al-OH-Si-OH	2 / Al-H_2O	18 / Al-OH-Si-OH

Table S14. Alumination energies obtained by decreasing the surface Si/Al ratio.* The surface Si/Al ratio is defined for the surface layer which depth corresponds to one bulk unit.

Surface Si/Al	Surface	Aluminated sites	Type of site	Illustration	$\Delta_r U_{al\_tot}$ (kJ.mol^{-1})	$\Delta_r U_{al\_theo}$ (kJ.mol^{-1})
23	(100) cleavage 1	Si_59 Si_63 Si_109 Si_117	Al-H_2O / 3 Al-OH-Si / 1 Al-OH-Si-OH / 1'' Al-OH-Si-OH / 1''	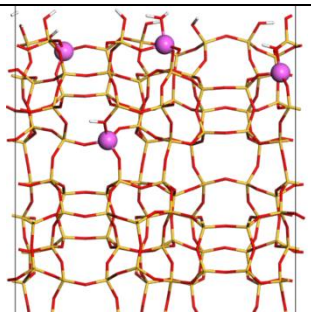	-138	-158
23	(100) cleavage 1	Si_59 Si_63 Si_109 Si_117	OH-Al-OH-Si / 1' Al-OH-Si / 1 Al-OH-Si-OH / 1'' Al-OH-Si-OH / 1''	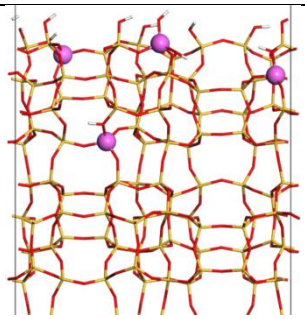	-100	-113
43	(101) cleavage 6	Si_37 Si_132	Al-H_2O / 3 Al-H_2O / 3	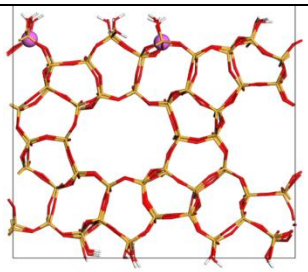	-144	-150
55	(101) cleavage 9	Si_57 Si_8	Al-H_2O / 3 Al-H_2O / 3	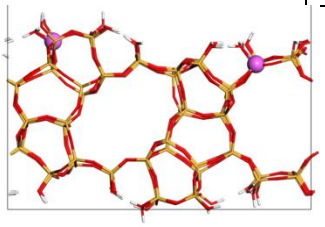	-205	-199

$* \Delta_r U_{al\_tot} = (U_{slab\_n\_Al} + nU_{Si(OH)_4} - U_{slab} - nU_{Al(OH)_3H_2O})$

$\Delta_r U_{al\_theo} = \sum_i \Delta_r U_{al\_i}$

with n the number of aluminated sites per unit cell, $U_{slab\_n\_Al}$ the energy of the surface with n aluminated sites, U_{slab} the similar but purely silicic surface and $\Delta_r U_{al\_n}$ the alumination energy defined in Eq. 2 of the silicon number n, this value can differ depending on the position of the proton.

SVII. Surface hydration/dehydration reactions

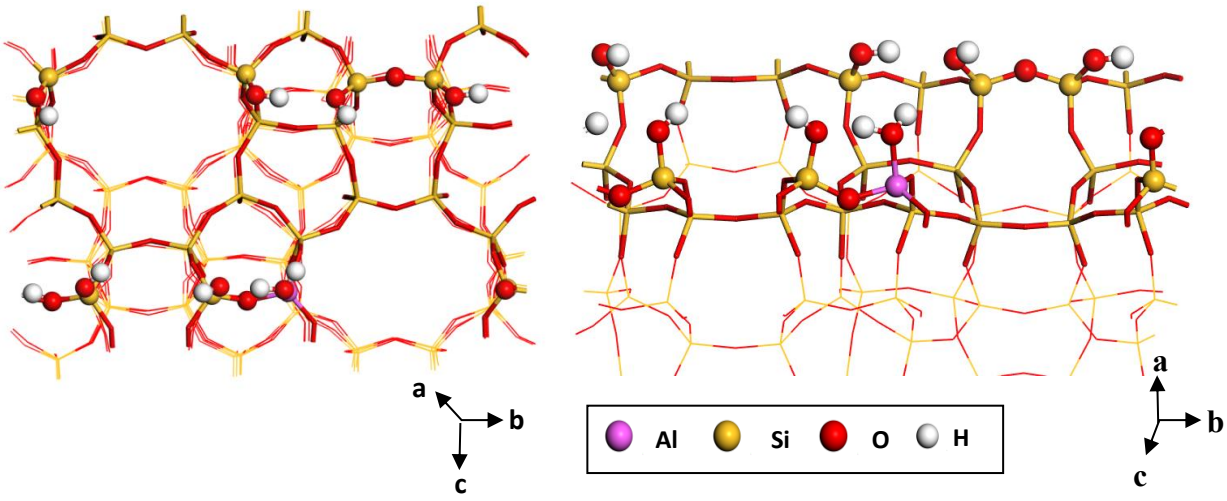

Figure S16. Surface of the initial surface for hydration and dehydration with 1.7 $H_2O.nm^{-2}$ (Left) Top view (Right) Side view. This surface exhibits 7 Si-OH groups and one Al-H_2O. The two pairs of Si-OH groups are close neighbors and form at the surface a HO-Si-O-Si-OH bridges.

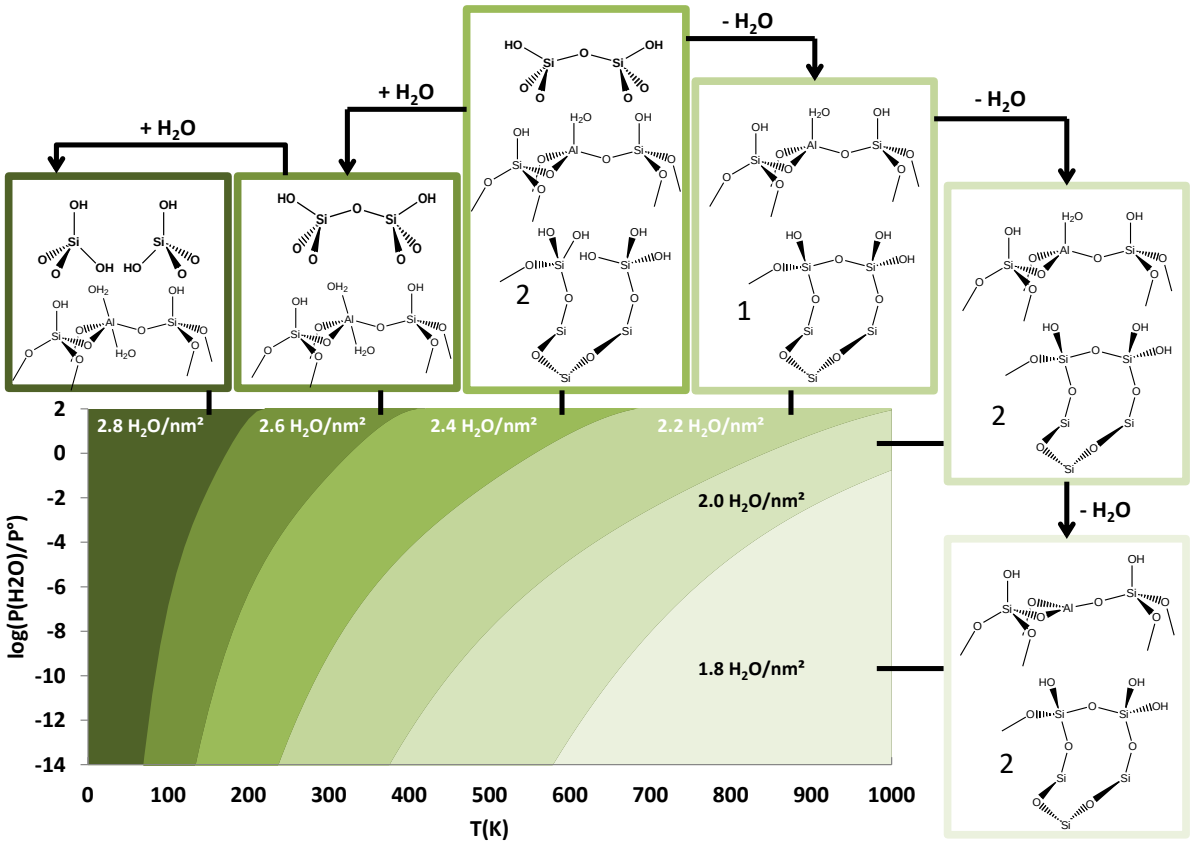

Figure S17. Surface hydration thermodynamic diagram for Al-(H_2O) site n°77 belonging to the cleavage 6 of (100) surface of ZSM-5

Table S15. Structures (Schematic view, top view and side view) of the systems invoked in Figure 6-a in the manuscript.

Hydration level ($H_2O.nm^{-2}$)	Schematic hydroxyl and aluminum groups	Surface	$\Delta_r U_{hyd}$ ($kJ.mol^{-1}$)
2.8	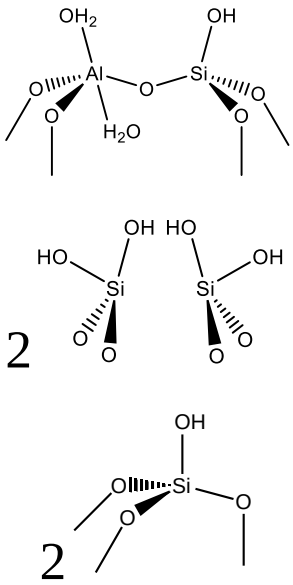	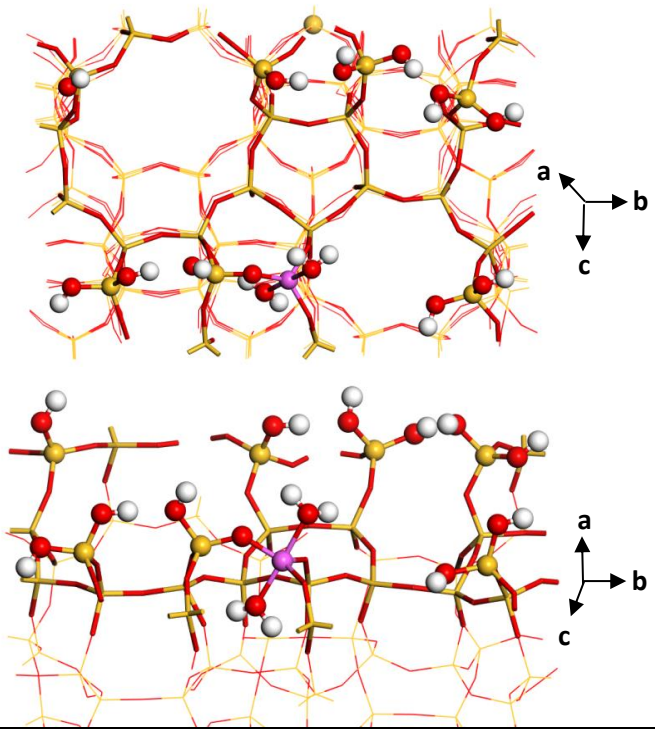	-95
2.1	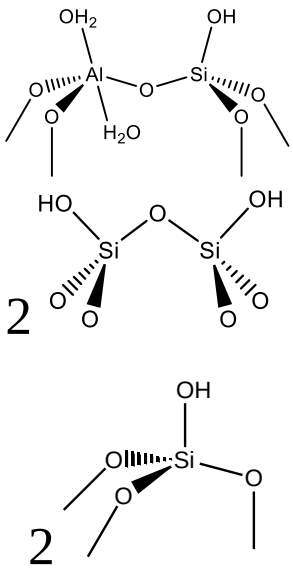	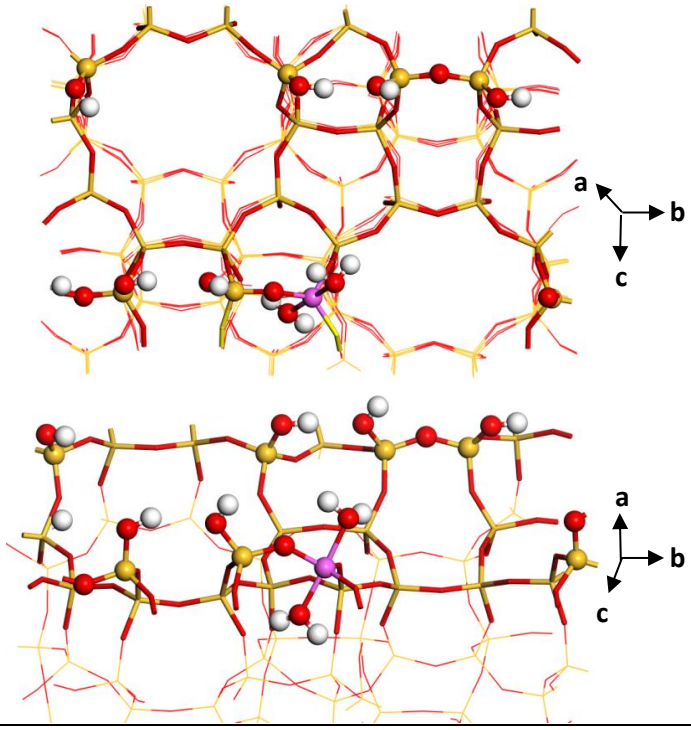	-56

1.3	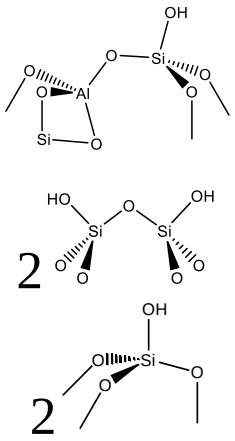	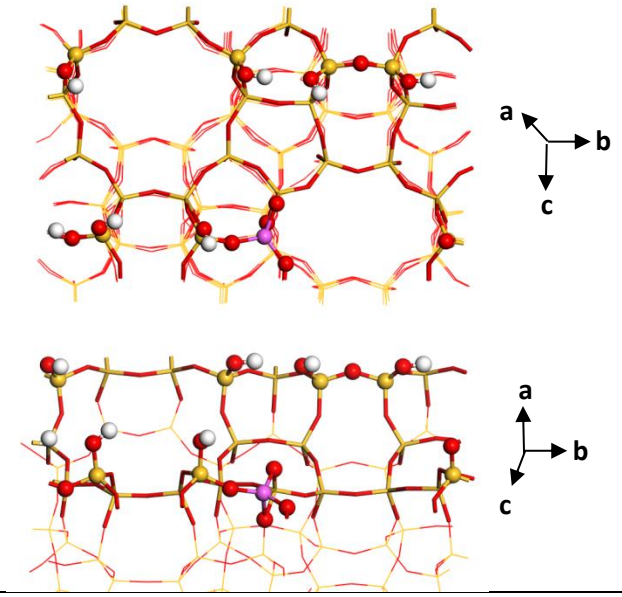	128
0.9	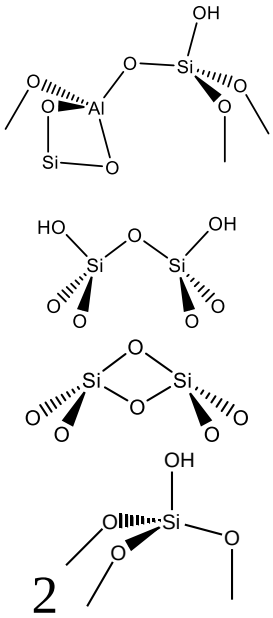	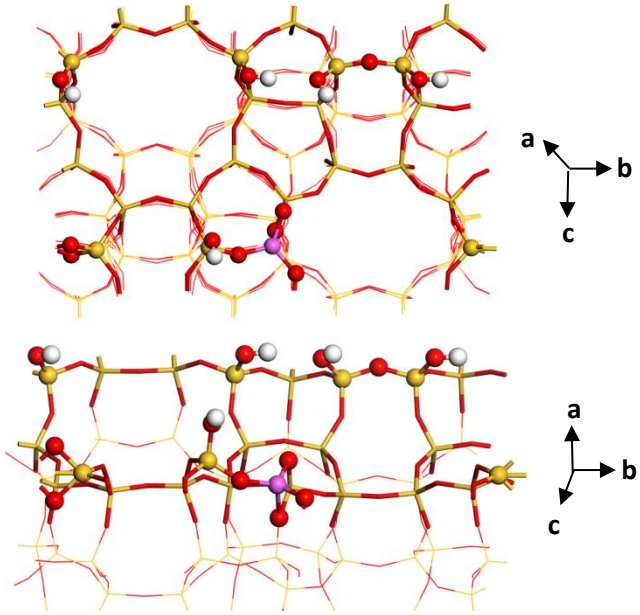	293
0.6	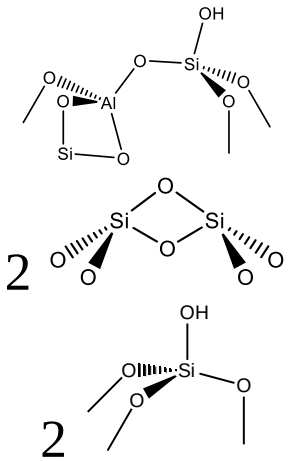	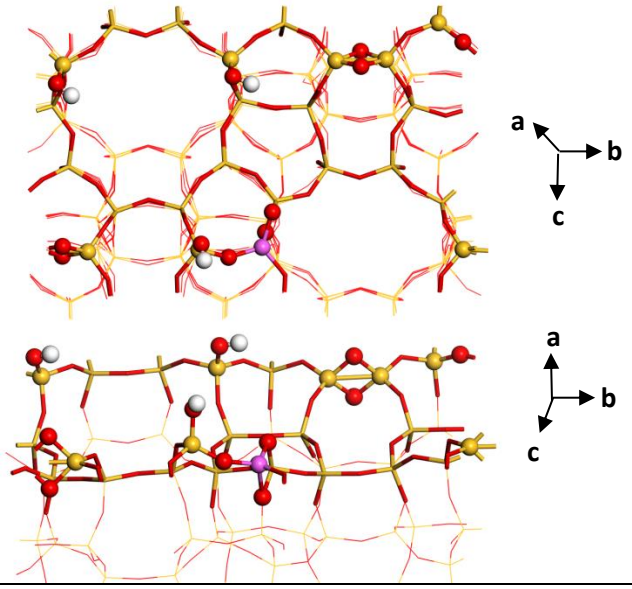	454

The electronic adsorption or desorption energy of each water molecule was calculated according to **Equation S1** and using the surface hydrated at 1.7 $H_2O.nm^{-2}$.

$$\Delta_r U_{hyd} = U_{hydrated\_slab} - U_{slab} -/+ n_{H_2O} U_{H_2O}$$

Equation S1

Table S16. Structures (Schematic view) of the systems invoked in Figure 6-b.

Hydration level ($H_2O.nm^{-2}$)	**Schematic hydroxyl and aluminum groups**	**$\Delta_r U_{hyd}$ (kJ.mol^{-1})**
2.1	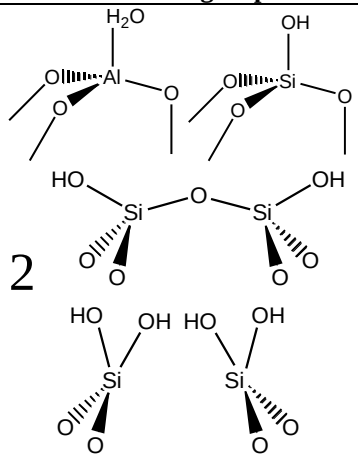	-13
1.7	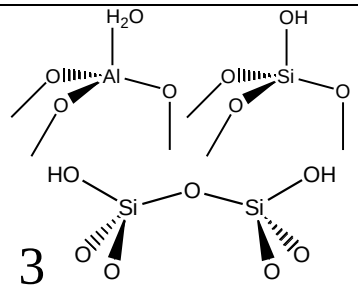	0
0.9	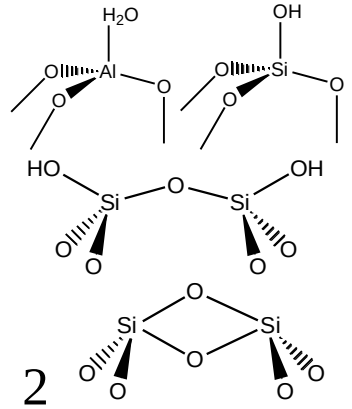	320
0.6	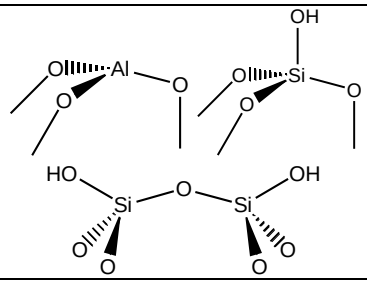	497

	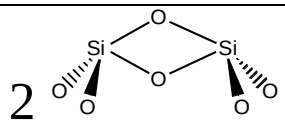 2	
0.2	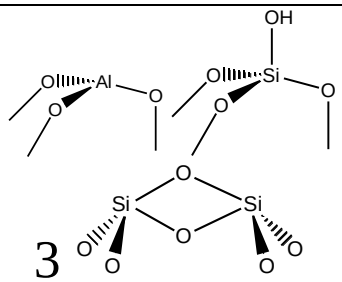 3	894

Table S17. Structures (Schematic view) of the systems invoked in Figure S17.

Hydration level ($H_2O.nm^{-2}$)	Schematic hydroxyl and aluminum groups	$\Delta_r U_{hyd}$ ($kJ.mol^{-1}$)
2.8	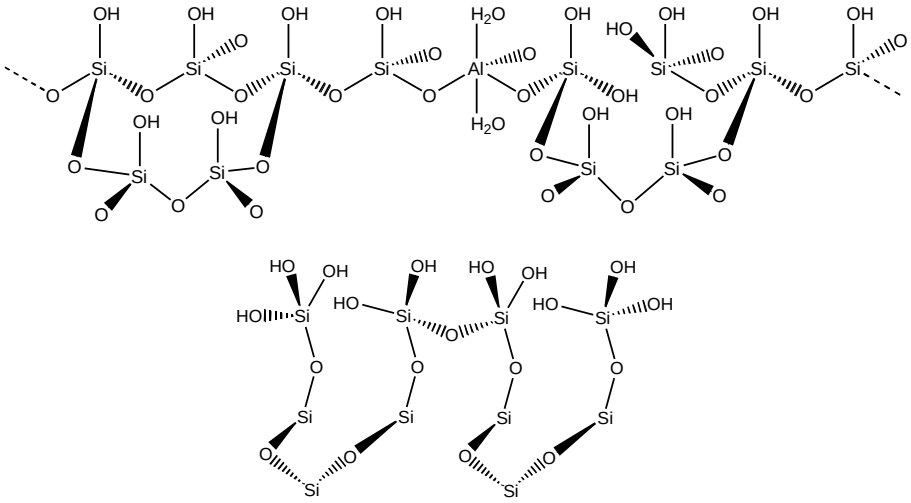	-80
2.6	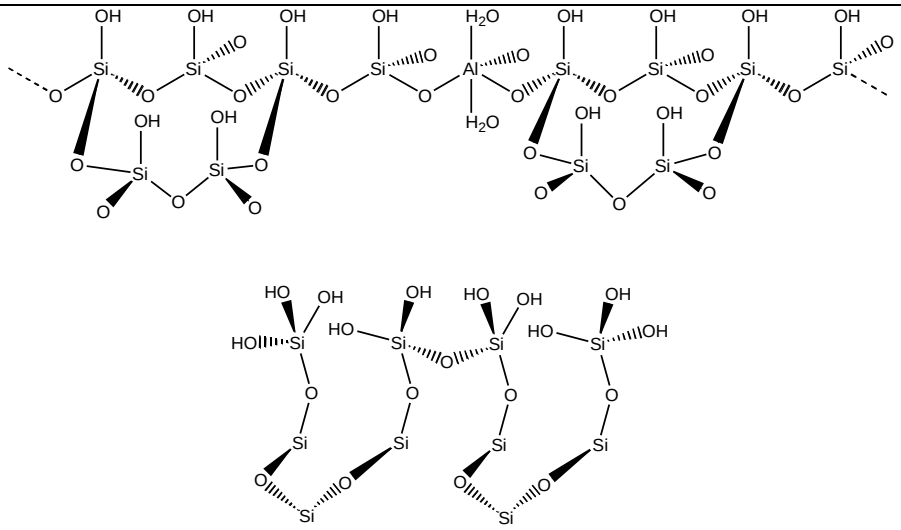	-54

2.4	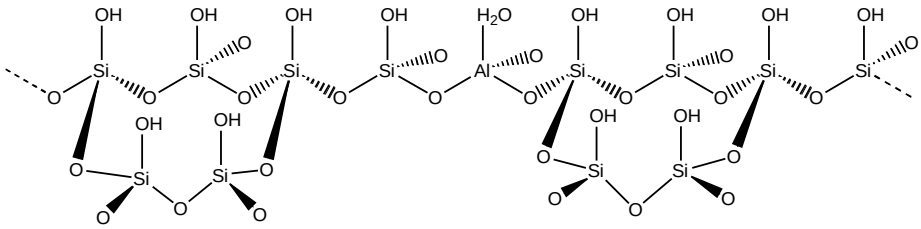 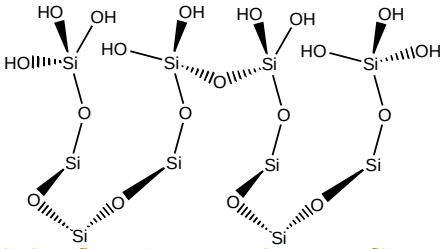 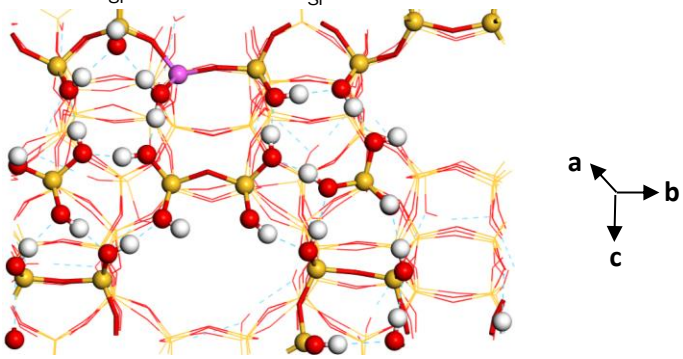 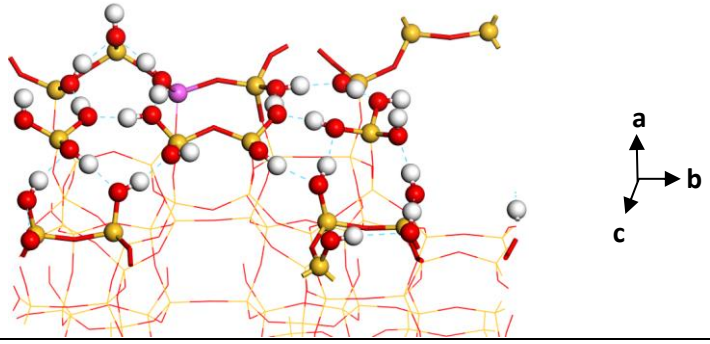	0
2.2	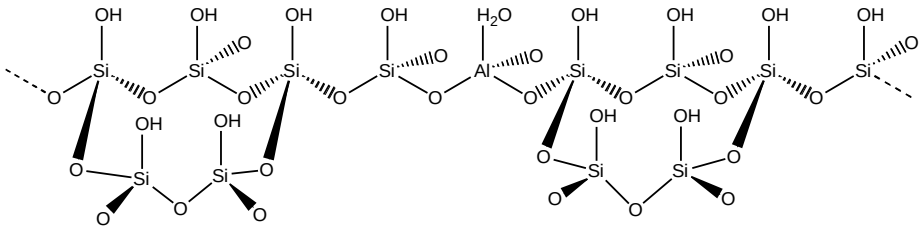 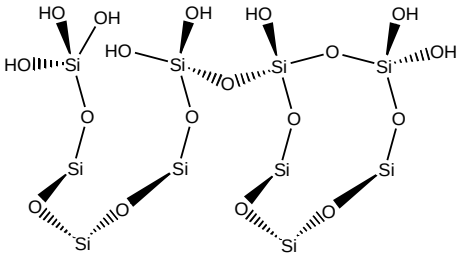	100

2.0	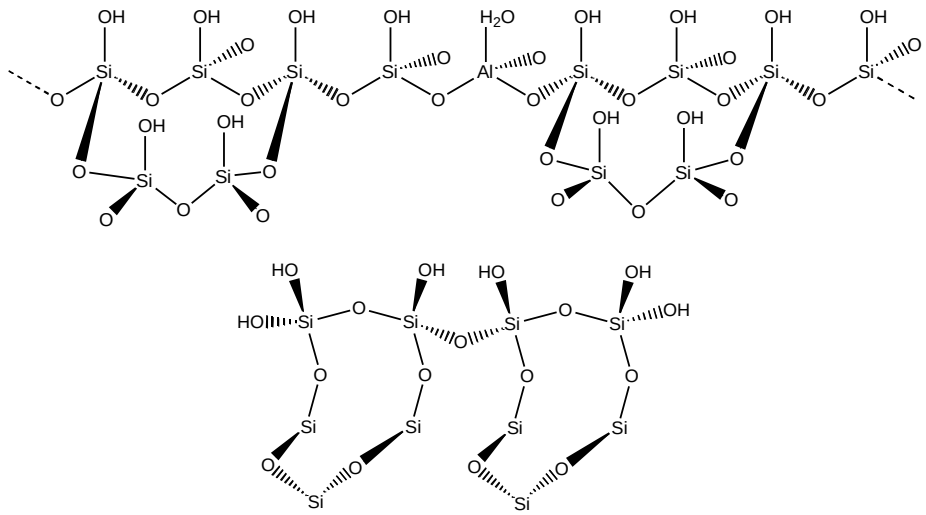	264
1.8	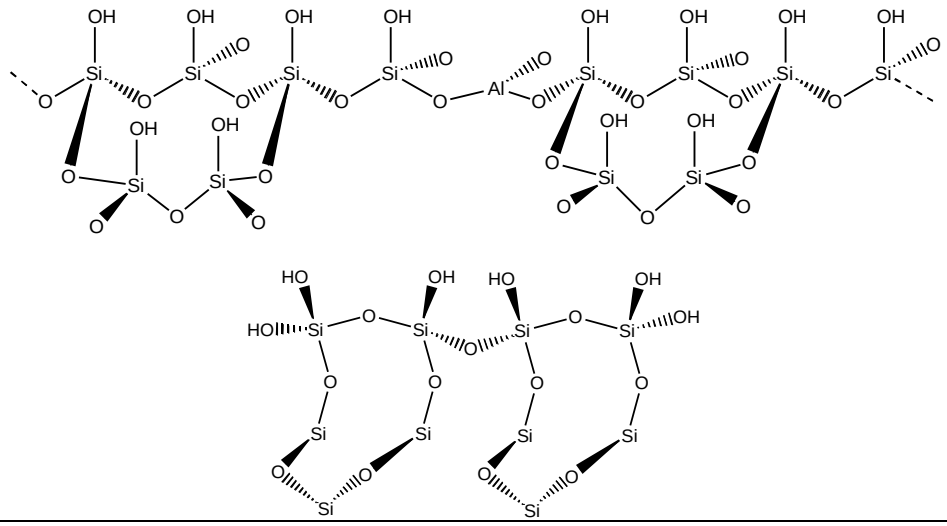	422

References

(1) Gruene, T.; Li, T.; van Genderen, E.; Pinar, A. B.; van Bokhoven, J. A., Characterization at the Level of Individual Crystals: Single-Crystal MFI Type Zeolite Grains, *Chem. Eur. J.* **2018**, *24*, 2384-2388.
(2) Zhai, D.; Liu, Y.; Zheng, H.; Zhao, L.; Gao, J.; Xu, C.; Shen, B., A First-Principles Evaluation of the Stability, Accessibility, and Strength of Brønsted Acid Sites in Zeolites, *J. Catal.* **2017**, *352*, 627-637.
(3) Li, C.; Vidal-Moya, A.; Miguel, P. J.; Dedecek, J.; Boronat, M.; Corma, A., Selective Introduction of Acid Sites in Different Confined Positions in ZSM-5 and Its Catalytic Implications, *ACS Catal.* **2018**, *8*, 7688-7697.